Research article

Open Access

Autologous chondrocyte implantation for cartilage repair: monitoring its success by magnetic resonance imaging and histology

Sally Roberts[1,2], Iain W McCall[3,2], Alan J Darby[4], Janis Menage[1], Helena Evans[1], Paul E Harrison[5] and James B Richardson[6,2]

[1]Centre for Spinal Studies, Robert Jones and Agnes Hunt Orthopaedic Hospital NHS Trust, Oswestry, Shropshire, UK
[2]Keele University, Keele, Staffordshire, UK
[3]Department of Diagnostic Imaging, Robert Jones and Agnes Hunt Orthopaedic Hospital NHS Trust, Oswestry, Shropshire, UK
[4]Department of Histopathology, Royal National Orthopaedic Hospital, Brockley Hill, Stanmore, Middlesex, UK
[5]Arthritis Research Centre, Robert Jones and Agnes Hunt Orthopaedic Hospital NHS Trust, Oswestry, Shropshire, UK
[6]Institute of Orthopaedics, Robert Jones and Agnes Hunt Orthopaedic Hospital NHS Trust, Oswestry, Shropshire, UK

Corresponding author: S Roberts (e-mail: s.roberts@keele.ac.uk)

Received: 29 July 2002 Revisions received: 18 October 2002 Accepted: 23 October 2002 Published: 13 November 2002

Arthritis Res Ther 2003, **5**:R60-R73 (DOI 10.1186/ar613)

Abstract

Autologous chondrocyte implantation is being used increasingly for the treatment of cartilage defects. In spite of this, there has been a paucity of objective, standardised assessment of the outcome and quality of repair tissue formed. We have investigated patients treated with autologous chondrocyte implantation (ACI), some in conjunction with mosaicplasty, and developed objective, semiquantitative scoring schemes to monitor the repair tissue using MRI and histology. Results indicate repair tissue to be on average 2.5 mm thick. It was of varying morphology ranging from predominantly hyaline in 22% of biopsy specimens, mixed in 48%, through to predominantly fibrocartilage in 30%, apparently improving with increasing time postgraft. Repair tissue was well integrated with the host tissue in all aspects viewed. MRI scans provide a useful assessment of properties of the whole graft area and adjacent tissue and is a noninvasive technique for long-term follow-up. It correlated with histology ($P = 0.02$) in patients treated with ACI alone.

Keywords: cartilage repair, collagens, glycosaminoglycans histology, MRI

Introduction

There is a burgeoning interest in cartilage repair worldwide, with particular focus on tissue engineering and cell-based therapies. While much effort goes into developing novel culture conditions and support mechanisms or scaffolds, autologous chondrocyte implantation (ACI) [1] remains the most commonly used cell-based therapy for the treatment of cartilage defects in young humans [2–4], although no randomised trials have been completed as yet [5]. Objective measures of the properties of the grafted regions are necessary for long-term follow-up of this procedure and to evaluate how closely the treated region resembles normal articular cartilage. Useful outcome measures that assess the overall function, structure, and composition of chondral tissue [6] include mechanical properties or its appearance in arthroscopy, histology, and magnetic resonance imaging (MRI), in addition to clinical assessment of the patient. However, there has been little standardisation of such outcome measures [7]. We have therefore developed histological and MRI scoring schemes and used them to assess the quality of repair tissue at varying time points up to 34 months after the grafting procedure. In addition, immunohistochemistry has been used to assess whether the tissue in the grafted site resembled normal articular cartilage, not only in its matrix organisation but also in its chemical composition.

3D = three-dimensional; ACI = autologous chondrocyte implantation; H&E = haematoxylin and eosin; ICC = intraclass correlation; MOD = modified O'Driscoll; MRI = magnetic resonance imaging; TE = echo time; TR = repetition time.

Cartilage function reflects its biochemical composition [8]. A small biopsy specimen such as is used for histochemical assessment can provide only limited information, as it is from a discrete location. MRI, in contrast, can provide information on the whole area. In addition, it is noninvasive and successive scans can be carried out, so allowing longitudinal monitoring at different time points. MR images have been shown to correlate with biochemical composition in other tissues, in cartilage *in vivo,* and even in engineered cartilage generated in a bioreactor [9–11]. Thus in this study we have used both forms of assessment of articular cartilage and correlated them where they are available at the same time points post-treatment. We have previously reported on the immunohistochemical appearance of such biopsy specimens, but only on two individuals and at 12 months after implantation [12]. Here we report on a much more extensive sample group, obtained up to 3 years after treatment, and compare histological assessments with those obtained by MRI.

Materials and methods

Tissue biopsies

Patients receiving ACI in our centre undergo arthroscopic assessment and biopsy of the treated region as part of their routine follow-up at approximately 12 months post-graft. The taking of biopsies from grafted regions was given ethical approval by Shropshire Research and Ethics Committee and all patients gave fully informed consent. Twenty-three full-depth cores of cartilage and subchondral bone were obtained from 20 patients (mean age 34.9 ± 9.2 years) who had undergone ACI [1,13] between 9 and 34 months previously (mean 14.8 ± 6.9 months). Six of these patients had been treated with ACI and mosaicplasty [osteochondral autologous transplantation (OATS)] combined, the rest with ACI alone. In the majority of patients, the femoral condyle was treated (11 medial, 6 lateral), in two the patella, and in one the talus (Table 1). Cores (1.8 mm in diameter) were taken from the centre of the graft region using a bone marrow biopsy needle (Manatech, Stoke-on-Trent, UK). A mapping system was used to ensure the correct location [14]. The cores were taken as near to 90° to the articulating surface as possible. The exception was patient 2, from whom the graft was taken obliquely in order to pass through a mosaic plug. Cores were snap-frozen in liquid-nitrogen-cooled hexane and stored in liquid nitrogen until studied. 'Control' samples of articular cartilage and underlying bone were obtained from three individuals, two from ankles of patients (aged 10 and 13 years) with non-cartilage pathologies and one from the hip (aged 6 years) obtained at autopsy. Ideally, normal tissue would have been taken that was matched for age and site, but unfortunately this was not available. In addition, meniscus from a 74-year-old woman was examined as an example of fibrocartilaginous tissue.

Magnetic resonance imaging

MRI was carried out before the follow-up arthroscopic procedure during which the biopsy specimen was taken. The following sequences were undertaken using a Siemens Vision 1.5T scanner (Siemens, Erlangen, Germany) with a gradient strength of 25 mT/m and VB33A software:

1. T_1 sagittal and coronal spin echo sequence. This provides information on the general anatomy of the joint, for example, identifying abnormalities in the menisci, cruciate ligaments, or other joint components and the subchondral bone outline and underlying marrow signal (repetition time [TR] = 722 ms; echo time [TE] = 20 ms; field of view = 20 cm; slice thickness = 3/0.3 mm; matrix 512 × 336; acquisition = 2).
2. A three-dimensional (3D) T_1-weighted image with fat saturation and a 30° flip angle. This provides information on the quality and thickness of the cartilage (TR = 50; TE = 11; flip angle = 30°; field of view = 18 cm; matrix 256 × 192; number of excitations = 1; slab = 90 mm; partitions = 60 [i.e. each slice = 1.5 mm]).
3. A 3D dual excitation in the steady state sequence with fat saturation. This demonstrates the surface characteristics of the cartilage and also highlights fluid in the joint and oedema in the subchondral bone (TR = 58.6; TE = 9; flip angle = 40°; field of view = 18 cm; matrix 256 × 192; number of excitations = 1; slab = 96 mm; partitions = 64 [i.e. each slice = 1.5 mm]; acquisition = 2).

The 3D images were acquired in the sagittal plane except in the patients with patella grafts, when images were acquired in the axial plane. These sequences allowed longitudinal study of the joint by comparison with previous scans carried out preoperatively, when a more extensive study also included obtaining a T_2-weighted gradient echo image in the sagittal and coronal planes and axial images with spin echo sequences.

For the purpose of the present study, a semiquantitative assessment has been developed, whereby each of four features considered important to the quality of the repair [15] are scored from the images. These can be seen in Table 2, together with the scores attributed to each feature. The scans were reviewed by one author, who was unaware of the histological evaluation.

Histology

Frozen sections 7 μm thick were collected onto poly-L-lysine-coated slides and stained with haematoxylin and eosin (H&E) and safranin O (0.5% in 0.1-M sodium acetate, pH 4.6, for 30 s) for general histology, measurement of cartilage thickness, and assessment of metachromasia. Cartilage thickness was measured as the perpendicular distance between the articular surface and the junction with the subchondral bone, thus eliminating errors that could occur in tangential biopsies. Sections were viewed

Table 1

Details of individuals from whom biopsy specimens were obtained and their histology and MRI scores

Patient and sample no.	Patient's age at ACI (years)	Sex	Interval between graft and biopsy (months)	Treatment	Location of defect or tissue source	OsScore (maximum 10)	MOD score (maximum 23)	MRI score (maximum 4)	Cartilage type	Thickness (mm)
1	20	M	11	M & ACI	MFC	9.5	21.2	1	H	3.2
2	20	F	11	M & ACI	LFC	7.0	18.3	1	H/F	1.4
3	25	M	16	ACI	LFC	4.7	14.3	0.5	F	6.2
4	28	M	12	ACI*	MFC	5.0	14.1	1	F	4.2
5	28	M	20		MFC	8.7	17.5	N/A	H/F	1.0
6	28	M	34		MFC	7.8	15.6	0	H	2.3
7	28	F	12	ACI	MFC	7.0	17.8	3	H/F	>2.5
8	28	M	11	ACI	MFC	6.0	16.3	3.5	H/F	3.0
9	29	M	12	ACI	MFC	6.3	16.8	2	H/F	>0.8
10	32	M	9	ACI	patella	4.0	7.2	2	F	1.8
11	32	M	12	ACI*	MFC	7.2	16.3	3	H/F	5.3
12	32	M	30		MFC	8.0	18.5	1.5	H/F	3.3
13	33	M	12	ACI	MFC	5.8	14.8	5	H/F	2.5
14	35	F	9	ACI	MFC	2.5	6.9	1	F	3.3
15	38	F	14	ACI	MFC	8.0	18.7	2	F	1.1
16	39	M	12	ACI	MFC	7.9	17.5	3	H/F	4.3
17	39	M	12	M & ACI	talus	9.7	20.2	0	H	>1.7
18	39	M	14	M & ACI	LFC	4.7	14.9	0	H/F	>1.0
19	41	M	12	ACI	LFC	5.8	16.2	2	F	1.1
20	42	F	12	M & ACI	LFC	7.6	17.9	3.5	H	1.6
21	45	F	12	M & ACI	patella	4.0	5.0	0	H/F	1.4
22	52	M	30	ACI*	LFC	9.7	18.1	2	H	1.6
23	53	F	12	ACI	MFC	5.2	14.8	4	F	2.0
24	6	F	n/a	Control	femoral head	9.2	18.6		H	2.3
25	10	F	n/a	Control	calcaneocuboid joint, ankle	9.3	21.0		H	1.5
26	13	M	n/a	Control	talonavicular joint, ankle	9.8	22.8		H	1.5
27	74	F	n/a	Control	meniscus				F	

*ACI carried out with cells grown in Carticel™; all others utilised OsCells, so-called because they were prepared in the laboratory in Oswestry.
ACI, autologous chondrocyte implantation; F, fibrocartilage-like; H, hyaline-like; LFC, lateral femoral condyle; M, mosaicplasty; MFC, medial femoral condyle; MOD, modified O'Driscoll; MRI, magnetic resonance imaging; n/a not applicable; N/A not available.

with standard and polarised light and images captured and digitised using a closed-circuit television and Image Grabber software (Neotech Ltd, Hampshire, UK).

A semiquantitative scoring system, the OsScore – so called because it originated in the laboratory in Oswestry (Table 3) – was devised, in which the following parameters were assessed: the predominant cartilage type present, the integrity and contour of the articulating surface, the degree of metachromasia with safranin O staining, the extent of chondrocyte cluster formation, the presence of vascularisation or mineralisation in the repair cartilage, and the integration with the calcified cartilage and underlying bone. The scores attributed to each of

Table 2

Features assessed for magnetic resonance image score

Feature	Score
Surface integrity and contour	1 = normal or near normal, 0 = abnormal
Cartilage signal in graft region	1 = normal or near normal, 0 = abnormal
Cartilage thickness	1 = normal or near normal, 0 = abnormal
Changes in underlying bone	1 = normal or near normal, 0 = abnormal
Maximum total possible	4

Table 3

Histological features measured for OsScore

Feature	Score
Tissue morphology	Hyaline = 3 Hyaline/fibrocartilage =2 Fibrocartilage =1 Fibrous tissue =0
Matrix staining	Near normal =1 Abnormal =0
Surface architecture	Near normal =2 Moderately irregular =1 Very irregular =0
Chondrocyte clusters	None =1 ≤25% cells = 0.5 >25% cells = 0
Mineral	Absent =1 Present = 0
Blood vessels	Absent = 1 Present = 0
Basal integration	Good = 1 Poor = 0
Maximum total possible	10

these parameters can be seen in Table 3. These properties were chosen for several reasons:

1. Morphology is thought to influence mechanical functioning of the tissue and is often of most interest to observers.
2. A smooth surface is important for articulation and in the transfer of incident loads throughout the underlying cartilage.
3. Metachromasia relates to proteoglycan content and hence load-bearing properties.
4. Clusters of chondrocytes in osteoarthritis are a negative feature associated with degeneration.
5. Vascularisation and mineralisation are both included as negative features, because they are not present in normal articular cartilage, but there is concern that they result from the periosteum used in the ACI procedure.
6. Integration to adjacent host tissue is of course an important feature, and therefore 'vertical' integration to the underlying bone is included.

Tissue type was categorised as predominantly (i.e. >60%) hyaline cartilage, predominantly (>60%) fibrocartilage, mixed (when there was a significant proportion of both hyaline and fibrocartilage present), or fibrous tissue. The tissue was classified as hyaline when it had the following properties: the extracellular matrix had a glassy appearance when viewed with polarised light, and the cells had a chondrocytic morphology, i.e. were oval, often with a pericellular capsule or lacuna apparent. In contrast, tissue was classified as fibrocartilage when bundles of collagen fibres were randomly organised and the cells were more elongated and often more numerous. Vascularisation and mineralisation were identified on H&E-stained sections, mineralisation being confirmed where necessary with von Kossa stain. For comparison with the OsScore, sections were scored using a modified O'Driscoll score (MOD; www.pathology.unibe.ch/Forschung/osteoart/osteoart.htm#project3), selecting the properties that it was possible to measure on isolated biopsy specimens. All samples were scored independently by three observers for both scoring systems. In both scoring systems, a high score indicates a good graft.

Immunohistochemistry

Immunostaining was carried out using monoclonal antibodies against collagens type I (clone no. I-8H5; ICN), II (CIICI, Developmental Studies Hybridoma Bank, Ohio, USA), III (clone no. IE7-D7; AMS Biotechnology Ltd, Abingdon, UK), and X [16]. A polyclonal antibody to type VI collagen was used [17]. Monoclonal antibodies against the glycosaminoglycans chondroitin-4-sulfate (2-B-6) [18], chondroitin-6-sulfate (3-B-3 [19] and 7-D-4 [20]), and keratan sulfate (5-D-4) [21] and against the hyaluronan-binding region on the aggrecan core protein (1-C-6) [22] were used.

Before immunolabelling, sections were enzymatically digested with hyaluronidase or chondroitinase ABC to unmask the collagen and proteoglycan epitopes, respectively [23,24], except for the unusually sulfated chondroitin-6-sulfate epitopes, 3-B-3(–) and 7-D-4, which had no pretreatment. Sections were fixed in 10% formalin before incubation with the primary antibody (before the enzyme digestion, in the case of the proteoglycan antibodies). Endogenous peroxidase was blocked with 0.3% hydrogen peroxide in methanol. Labelling was visualised with peroxidase and the chromagen diaminobenzidine as the substrate, with avidin–biotin complex (Vector Laboratories, Peterborough, UK) being used to enhance labelling of monoclonal antibodies.

Table 4

Summary of scores according to morphology of cartilage

Cartilage type	Number	Time point post ACI (months)	Thickness (mm)	OsScore	MOD score	MRI score
In graft patients						
Hyaline-like	5	19.8 ± 11.2	2.1 ± 0.7	8.9 ± 1.1	18.6 ± 2.2	1.3 ± 1.5
H/F mixed	11	14.4 ± 5.8	2.4 ± 1.5	6.6 ± 1.4	15.8 ± 3.8	1.8 ± 1.1
Fibrocartilage-like	7	12.0 ± 2.5	2.8 ± 1.9	5.0 ± 1.7	13.2 ± 4.5	1.6 ± 1.6
In controls						
Hyaline-like (except fibrocartilage meniscus)	3		1.8 ± 0.5	9.4 ± 0.3	20.8 ± 2.1	N/A

ACI, autologous chondrocyte implantation; H/F, hyaline/fibrocartilage; MOD, modified O'Driscoll; MRI, magnetic resonance imaging; N/A, not available; OsScore, score devised in the laboratory in Oswestry.

Statistics

Nonparametric tests, the Mann–Whitney *U* test and Spearman rank correlations, were carried out using the Astute software package (Analyse-it Software Ltd, Leeds, UK). Intraclass correlation coefficients (ICC 2,1) were calculated to assess the reproducibility of the histology scoring systems by independent observers [25].

Results

Graft morphology and histology scores (Table 4)

The thickness of the cartilage in the patient biopsy specimens ranged from approximately 0.8 mm to 6.2 mm (mean 2.5 ± 1.5 mm), whereas in the control samples it was 1.8 ± 0.5 mm (range 1.1–2.1 mm). The cartilage morphology was predominantly hyaline (>90%) in five of the biopsy specimens and predominantly fibrocartilage in seven, and the remaining 11 biopsy specimens had areas with both hyaline and fibrocartilage morphology ('mixed'). The controls, in contrast, were all of hyaline morphology except for their fibrocartilaginous meniscus. The histology scores ranged from 2.5 to 10 (OsScore) and from 6 to 22 (MOD), with the mean OsScores being 8.9, 6.6, and 5.0 for hyaline, mixed, and fibrocartilaginous morphologies, respectively (see Table 4). Mean MOD scores were 18.6, 15.8, and 13.2 for these groups. There was a correlation ($r = 0.9$, $P < 0.001$) between the two scoring systems for all the 26 cartilage samples. Consistency of scoring between the three observers was higher for the OsScore (ICC = 0.77) than for the MOD score (ICC = 0.52) and the OsScore had an intraobserver error of 6% coefficient of variance. The mean thicknesses for the hyaline, mixed-morphology, and fibrocartilage cores were 2.1, 2.4, and 2.8 mm, respectively (see Table 4). The mean interval between graft and biopsy for the three groups ranged from 19.8 months to 12.0 months (see Table 4).

Integration of tissue in the grafted region with adjacent tissue appeared complete as far as could be assessed. Certainly 'vertical integration' looked good, with continuous fibres usually visible from the noncalcified cartilage through the calcified cartilage to the underlying bone (Fig. 1a,b). Lateral integration is more difficult to assess in small biopsy specimens such as those used in this study. However, in one patient treated with ACI and mosaicplasty combined, a specimen was taken obliquely. The morphology of the core suggests that it included a transplanted mosaic plug that was clearly hyaline and adjacent repair tissue that was fibrocartilaginous (Fig. 1c–g). The interface between these two regions, however, was fully integrated, as seen both in polarised light and on immunostaining for collagens (Fig. 1c–g).

MRI

The mean time in days between biopsy and MRI scan was 15.5 ± 12.3 days, apart from two samples for which there were intervals of 76 and 110 days.

On MRI, the thickness of the graft cartilage appeared the same as that of the adjacent cartilage in 68% of patients. The surface of the articular cartilage was smooth in 26% of patients (Fig. 2) and the remaining 74% showed some unevenness, irregularity, or overgrowth at the surface. Seven patients had subchondral cysts evident on their MRI scans, two of them having been treated with mosaicplasty and ACI combined. The cyst in one patient was obvious preoperatively and so was known to be unrelated to the ACI procedure. Five of the six patients treated with ACI and mosaicplasty combined scored 0 for the bone parameter. In some patients, artefacts were visible, for example, from previous interventions, but none affected the assessment of the graft region in this study. There were instances of all MRI scores possible (up to a maximum of 4) but there was no general trend with respect to cartilage morphology group (see Table 4). When all the samples were considered together, there was no significant correlation between the MRI score and the histology scores obtained at the same (or similar) time

Figure 1

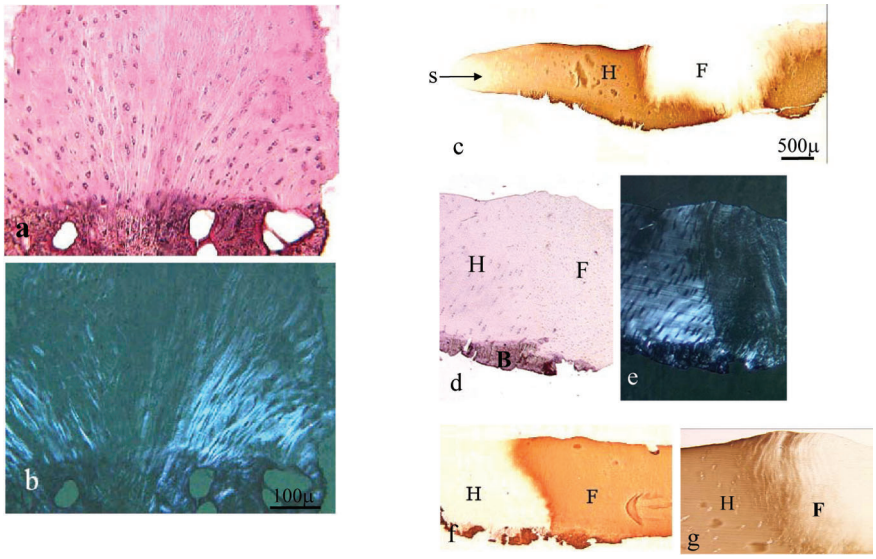

Integration between repaired cartilage and underlying bone, seen particularly clearly when a section stained with H&E **(a)** is viewed with polarised light **(b)** (sample 4). **(c)** An oblique section from the surface zone (S) through hyaline cartilage of the mosaic plug (H) to fibrocartilage matrix (F), immunostained for type II collagen. **(d)** H&E-stained higher power of the junctional zone (B, underlying bone) and **(e)** the same section viewed with polarised light. Full integration can be seen across this zone in sections immunostained for **(f)** type I and **(g)** type II collagen (sample 2). H&E, haematoxylin and eosin.

point. However, if samples from patients with combined ACI and mosaicplasty were excluded and only those from patients treated with ACI alone were considered, there was a significant correlation ($r = 0.6021$, $P = 0.02$, $n = 14$) between their MRI scores and OsScores. The individuals treated with ACI and mosaicplasty combined had lower MRI scores (mean 0.9 ± 1.4) than those treated with ACI alone (mean 2.0 ± 1.1), the overall mean for all patients being 1.7 ± 1.2.

Immunohistochemistry

Staining for type II collagen was positive in all specimens with hyaline morphology, although sometimes the uppermost layer (up to 300 µm) was negative. In most specimens with mixed or fibrocartilage morphology, 50% or more of the matrix was positive (Fig. 3; Table 5). There were few exceptions to this, with two fibrocartilage specimens being totally negative for type II collagen. Type I collagen immunostaining was seen in all samples but was more variable than for type II collagen. In the fibrocartilage-like samples, the staining was widespread throughout the matrix, whereas in those with hyaline morphology, its distribution was discrete and usually restricted to the very uppermost region, approximately 250 µm thick for the specimens from ACI-treated patients (Fig. 4). Staining for type X collagen occurred in 62% of samples, but when present it was only in small areas, usually in and around cells in the deep zone, close to the calcified cartilage or bone and the tidemark (Fig. 5). There was immunostaining for collagen types III and VI in all samples studied except for one, which was negative for type VI collagen. The distribution, however, differed markedly depending on the morphology of the matrix. In fibrocartilage, staining for collagen types III and VI was homogeneous throughout, whereas in hyaline cartilage it was clearly cell-associated, staining the cell and pericellular matrix but not the interterritorial matrix (Fig. 6).

Of the proteoglycan components, the strongest staining was for chondroitin-4-sulfate (with 2-B-6), which was throughout virtually all the matrices. Staining for the keratan sulfate epitope (with 5-D-4) was also common, particularly in hyaline cartilage. For the chondroitin-6-sulfate epitope (stained with 3-B-3), however, the distribution was often as for types III and VI collagens, predominantly homogeneous in fibrocartilage but more cell-associated in the hyaline cartilage. There was much less staining for the unusually sulfated chondroitin-6-sulfate epitopes, with 7-D-4 and, especially, 3-B-3(–), which was seen only occasionally; when present, it tended to be cell-associated in the hyaline regions (Fig. 7).

Hyaline 'control' cartilage was immunopositive virtually throughout for type II collagen, negative regions, if any, being restricted to a very thin strip (<50 µm) at the surface and the underlying bone (Fig. 8). The opposite was true for type I collagen, being negative apart from the bone and sometimes a very thin layer at the surface (see Fig. 8). Staining for types III and VI collagens was cell-associated and for type X collagen was restricted to the

Figure 2

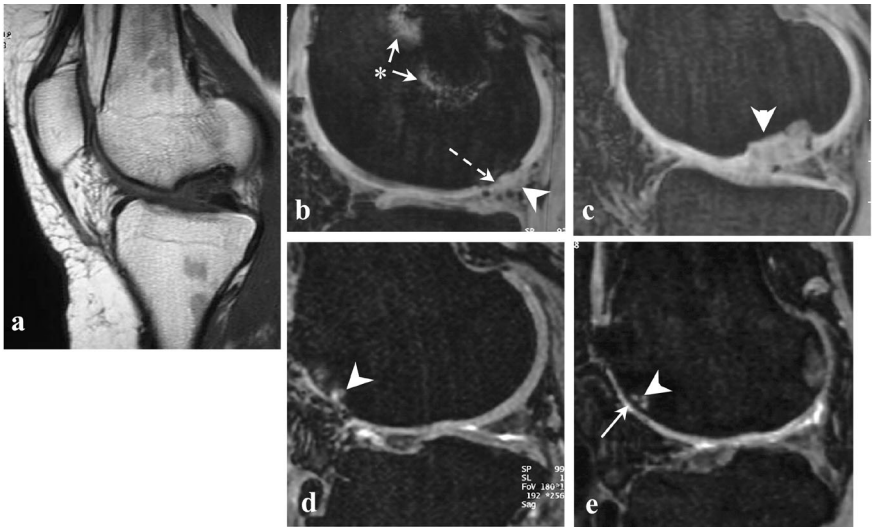

Use of MRI after ACI in joints. **(a)** The status of the whole knee (sample 7, sagittal T_1-weighted spin echo, TR = 722, TE = 20, field of view = 20 cm). **(b)** Cartilage surface congruity and cartilage overgrowth (arrowhead, sample 3) and **(c)** cartilage filling a subchondral defect (arrowhead, sample 7) can be identified on 3D T_1-weighted images with fat suppression. Similarly, the images can demonstrate changes in the bone, whether uneven bone profile (b) (dotted arrow), cysts in the underlying subchondral bone **(d,e)** (arrowheads), or artefacts (b) (asterisk). MRI is particularly suitable for longitudinal study of grafts such as can be seen in (d) and (e), which were taken at, respectively, 6 and 30 months after ACI treatment (sample 22, 3D dual excitation in the steady state with fat suppression). 3D, three-dimensional; ACI, autologous chondrocyte implantation; MRI, magnetic resonance imaging; TE, echo time; TR, repetition time.

Figure 3

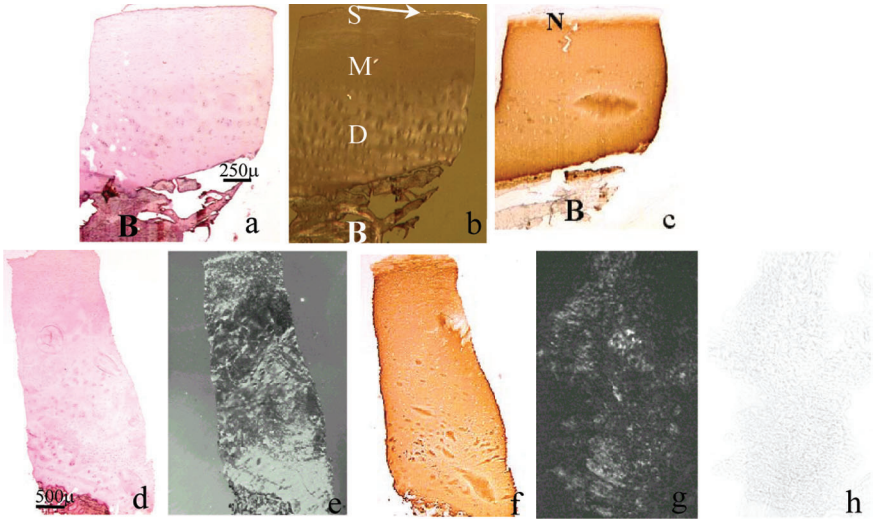

Immunohistochemical study of type II collagen after autologous chondrocyte implantation. Type II collagen is seen throughout most hyaline-like repair tissue **(c)**, as identified on an adjacent section stained with H&E **(a)** and viewed with polarised light **(b)**, showing zonal matrix organisation similar to that seen in normal adult articular cartilage in the surface (S), mid (M), and deep (D) zones (sample 22). In (c), note the lack of staining for type II collagen both at the surface (N) and in the bone (B). Samples with a mixed morphology **(d–f)** (sample 16) and some with a fibrocartilage morphology were mostly stained positively for type II collagen also, whereas a few fibrocartilagenous biopsy specimens **(g)** (sample 14) were negative for type II collagen **(h)**. H&E, haematoxylin and eosin.

deep zone and tidemark, except in sample 24, which had slight staining in the upper surface zone. The glycosaminoglycan epitopes that stained most strongly were keratan sulfate and chondroitin-4-sulfate. Less staining was seen for chondroitin-6-sulfate, with very slight staining for the unusually sulfated epitope, demonstrated with 7-D-4. The

Table 5

Summary of immunohistochemistry results demonstrating how the distribution of different epitopes varies with morphology, ranging from normal articular cartilage through to fibrocartilage

Collagen or glycosaminoglycan epitope	'Normal' articular cartilage	Hyaline-like repair tissue	Hyaline/ fibrocartilage repair tissue	Fibrocartilage-like repair tissue	Meniscus (fibrocartilage)
Collagen					
I	–	–	–/+	+	++
II	++	++	+	+	+/–
III	+pc	+pc	+pc/+	+	++
VI	+pc	+pc	+pc/+	+	+pc
X	+pc	+pc	+pc/–	–	–
Glycosaminoglycan					
Chondroitin-4-sulfate: (2-B-6)	++	++	+	+	++
Chondroitin-6-sulfate: (3-B-3)	+	++pc	+pc/(+)	++	+
Chondroitin-6-sulfate: (3-B-3(–))	(+)/–	(+)/–	+/–	(+)/–	–
Chondroitin-6-sulfate: (7-D-4)	+	(+)	–/(+)	–	–
Keratan sulfate: (5D4)	++	+(+)	+/(+)	+	(+)

– None or negligible (5% of section area); (+) slight; + some; ++strong; pc pericellular.

Figure 4

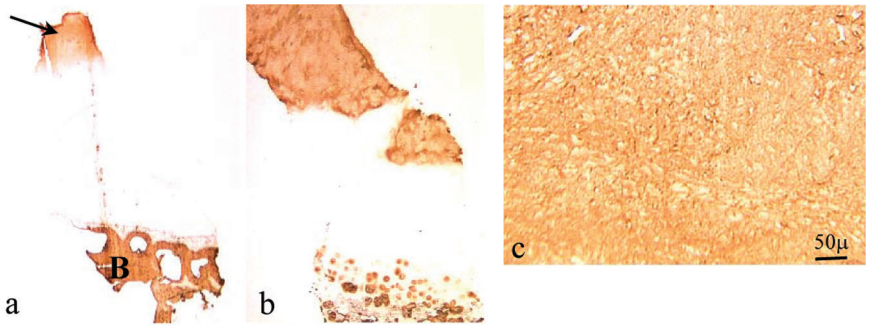

Immunostaining for type I collagen after autologous chondrocyte implantation.Type I collagen was restricted primarily to the upper region (arrow) and bone (B) in hyaline-like cartilage **(a)** (sample 22) but was more widespread where the morphology was mixed **(b)** (sample 16) or particularly when it was fibrocartilaginous **(c)** (sample 14).

meniscus, in contrast, had much staining for types I and III collagens, patchy staining for type II collagen, and a little for type VI collagen. Most glycosaminoglycan staining was for chondroitin-4-sulfate, with less for keratan sulfate than other samples, and no staining with antibodies 3-B-3(–) or 7-D-4 present.

Discussion

Although ACI has been carried out as a treatment for cartilage defects for 14 years [26], there remains much discussion about the efficacy of the procedure, despite 74–90% of patients having good to excellent results clinically in a 2–10-year follow-up study of more than 200 patients [27]. Objective outcome measures are required to assess any form of treatment and to date there is a substantial lack of information on the biochemical nature of cartilage repair tissue [28]. We have used MRI and histology as a means of assessing the quality of repair tissue in patients treated with ACI, sometimes in conjunction with mosaicplasty. In an attempt to render the observations more objective and, to some extent, quantitative, we have designed scoring systems specifically for patients who have had cartilage repair. Immunohistochemistry has been used to facilitate some assessment of the biochemical components within the repair tissue.

Figure 5

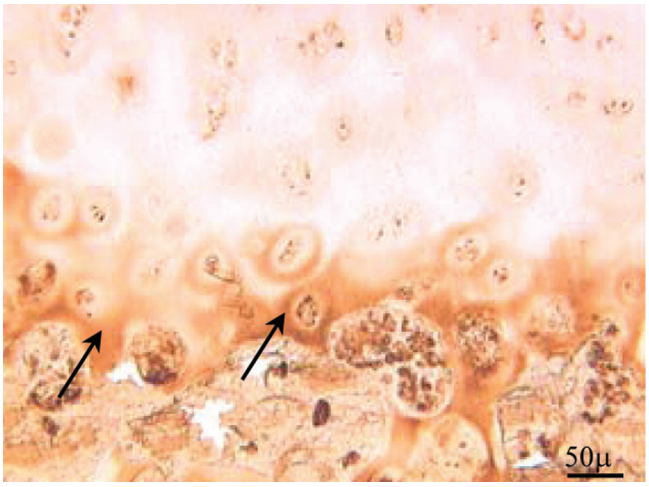

Immunostaining for type X collagen after autologous chondrocyte implantation. Staining was typically seen around the cells in the deep zone (arrows) and calcified cartilage (sample 16).

Many histological scoring systems have been published, but these have primarily been designed for animal studies of cartilage repair in rabbits [29–35] or dogs [36]. The scores assess parameters such as cell and tissue morphology, degree of chondrocyte clustering, surface regularity, structural integrity, thickness, metachromasia, bonding to adjacent cartilage, filling of the defect, and degree of cellularity. Some of these parameters can be assessed only on whole joints, which are commonly available in the animal models but not appropriate for humans. Here, where histological examination is carried out on biopsy specimens of the repair tissue, these specimens must be as small as possible and usually obtained only at one time point (thereby having certain inherent limitations, e.g. only representing a small area at one location within the treated area). Scoring systems for human tissue have been published, but these have, in the main, been devised for studies on osteoarthritis [37,38]. Hence many of the parameters assessed, such as growth of pannus, may be inappropriate for cartilage repair. Thus, in this study we have devised a histology score specifically for small, discrete biopsy specimens obtained from human patients undergoing treatment to induce repair of cartilage. We have identified characteristics that, in our opinion, are important to monitor and assess the quality of repair tissue. These include features such as the presence of blood vessels or mineralisation, in addition to the more obvious parameters such as integration with the underlying bone and tissue morphology. Other features should perhaps be considered for inclusion in the assessment procedure, such as the predominant type of collagen present or whether a higher degree of matrix organisation is present; i.e. whether hyaline cartilage has developed the zonal organisation typical of adult articular cartilage. While the latter is easily identifiable and could be included in the scoring scheme, the former is not necessarily routinely available in all support laboratories.

Nonetheless, it was felt to be of some benefit to compare the purpose-devised scoring system to one previously devised and described in the literature. Therefore, a scoring system used by many groups researching cartilage repair was chosen: the modified O'Driscoll (MOD) score. This utilises parameters identified by O'Driscoll *et al.* [29] in their study of periosteal grafts to treat cartilage defects in rabbits. The correlation between the modified

Figure 6

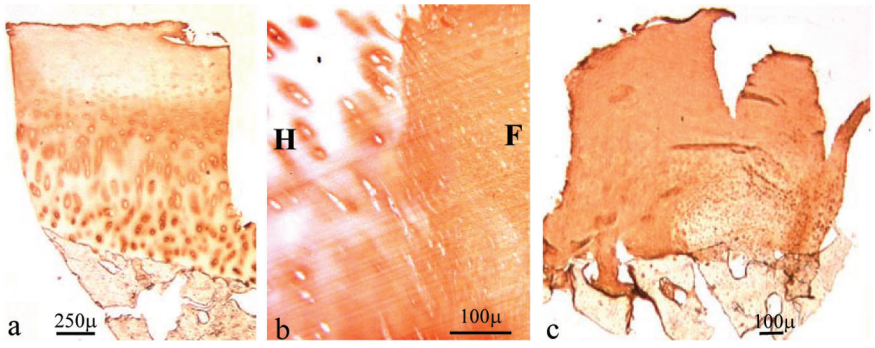

Immunostaining for type III collagen after autologous chondrocyte implantation. The distribution of type III collagen was predominantly pericellular in hyaline-like cartilage **(a)** (sample 22) and **(b)** (H) (sample 2), whereas in specimens with a more fibrocartilaginous morphology **(b)** (F) (sample 2) and **(c)** (sample 15), it was predominantly homogeneous throughout the extracellular matrix.

Figure 7

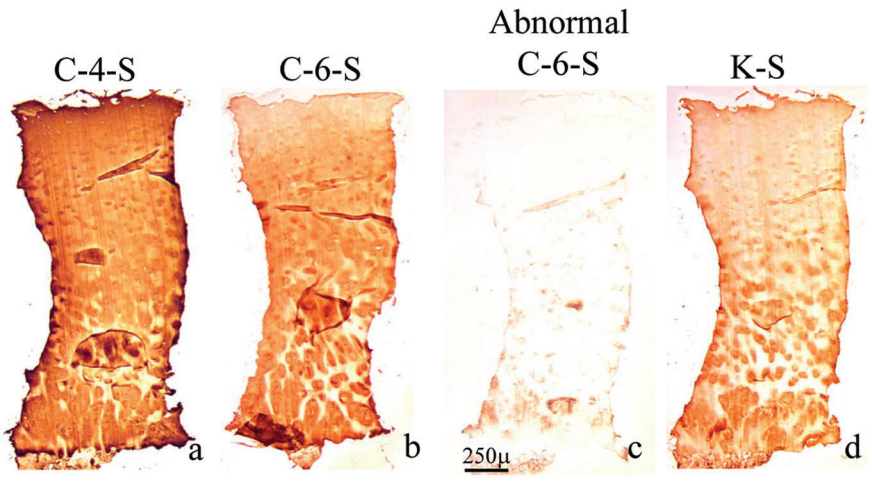

Immunostaining for glycosaminoglycan epitopes after autologous chondrocyte implantation. Staining was stronger for chondroitin-4-sulfate (2-B-6) **(a),** chondroitin-6-sulfate (3-B-3) **(b)**, and keratan sulfate (5-D-4) **(d)** than for the abnormally sulfated chondroitin-6-sulfate epitopes, 3-B-3(–) **(c)** (sample 6). C-4-S, chondroitin-4-sulfate; C-6-S, chondroitin-6-sulfate; K-S, keratan sulfate.

Figure 8

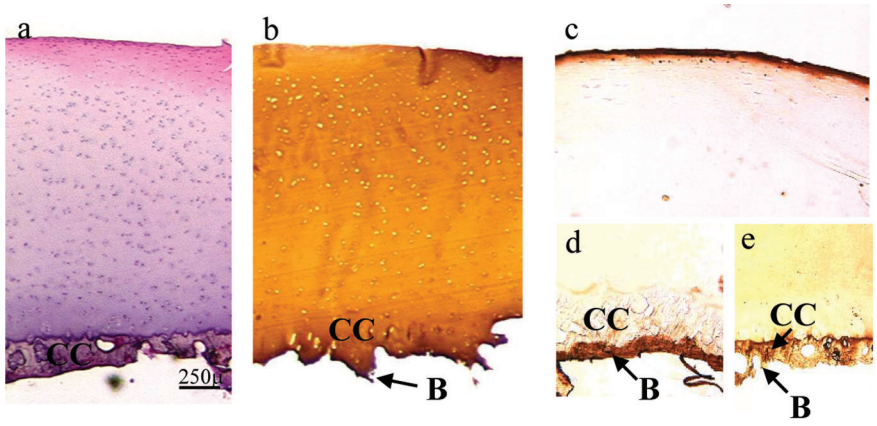

Typical staining and immunostaining patterns for control cartilage. Haematoxylin and eosin **(a)**, type II collagen **(b)**, type I collagen in the surface zone **(c)** and the deep zone **(d)** and type X collagen **(e)**. B, bone; CC, calcified cartilage.

O'Driscoll score (but restricted to the parameters that could be assessed on small core biopsy specimens) and the OsScore was reasonable ($r = 0.91$, $P = 0.0001$, $n = 26$) and they could be deemed to achieve their purpose, in that control samples of 'normal' hyaline tissue scored 94 ± 3% of maximum for OsScore and 90 ± 9% for the MOD score. However, all three observers found the OsScore much easier, quicker, and more reproducible to use.

Other workers have reported that hyaline cartilage is often formed in people treated by ACI [26,27]. In the present study, three of the five samples showing hyaline cartilage morphology were from individuals treated with ACI and mosaicplasty combined. If the biopsy specimen was taken through a transplanted mosaic plug (which makes up approximately 80% or more of the treated area), one would expect it to be hyaline cartilage. The other two specimens that were hyaline cartilage were both obtained much longer after the ACI treatment (30 and 34 months) than 16 of the 17 other cores. In addition, the average time interval between graft and biopsy was greatest for biopsies of hyaline morphology (19.8 months) and least for those of fibrocartilage morphology (12.0 months). This suggests that the cartilage that forms initially is often more fibrocartilaginous but may transform with time to remodel to form hyaline cartilage, possibly in response to loading. The appearance of zonal organisation (sample 22) typi-

cally found in normal adult articular cartilage suggests that this technique can indeed lead to regeneration of articular cartilage and may not require the use of a scaffold as is necessary in animal models [39].

The most ubiquitous type of collagen in normal adult articular cartilage is type II [40], both in calcified and uncalcified tissue [41]. The fact that this was commonly found in all but two samples of repair tissue in the present study is encouraging, even though production of type II collagen is not exclusive to hyaline cartilage and is also produced by some fibrocartilages such as the intervertebral disc [42]. The other collagen types examined in the present study (types I, III, VI, and X) have all been described in normal articular cartilage [40,43]. Collagen types III and VI are typically pericellular, particularly in the deep zone [43,44] as was found in hyaline cartilage in the biopsy specimens in the present study. Type I collagen has also been reported in articular cartilage: in the normal tissue it is usually restricted to the upper surface layer and the bone, similar to that found in the control samples (see Fig. 8). Similarly, type X collagen has been found in normal articular cartilage, predominantly in the deep zone and sometimes in the surface layer [45]. All of these collagen types – I, III, VI, and X – have been reported to occur at increased levels in diseased cartilage such as osteoarthritis [44,46,47]. The presence of type X collagen is considered by some people to be undesirable as it is found in the growth plate, for example, in the hypertrophic zone, which goes on to calcify. However, it is also found in extracellular matrices in cartilage [45] and intervertebral disc [48], which do not often proceed to mineralisation.

Chondroitin sulfate and keratan sulfate glycosaminoglycans are typically found in both articular cartilage [49] and fibrocartilage [50], their distribution and intensity varying with age and stage of development. The presence of 7-D-4 in 'control' hyaline cartilage seen here is likely to reflect the youth of the control subjects, as other studies have shown this and other abnormally sulfated chondroitin-6-sulfate epitopes to be expressed in developing and growing articular cartilage [51]. Lin *et al.* [52] found the expression of 7-D-4 to be greatest of all the proteoglycan epitopes in repair tissue in animal models of cartilage repair. They found it was able to differentiate repair hyaline tissue from both normal and fibrous repair tissue. Certainly in the present study there was no staining with the antibody 7-D-4 in totally fibrocartilaginous samples (either the ACI biopsy specimens or the meniscus).

MRI is considered by some to be the optimal modality for assessing articular cartilage [11,53], being able to evaluate the volume of repair tissue filling the cartilage defect, the restoration of the surface contour, the integration of the repair tissue to the subchondral plate, and the status of the subchondral bone [11]. MRI can reliably detect overgrowth or hypertrophy or graft delamination. It can also detect oedema-like signal in the marrow underlying the autologous chondrocyte repair. The significance of these marrow changes has yet to be clarified, but persistent or increasing oedema-like signal may indicate that the repair tissue is failing.

The use of MRI is limited to some extent, however, by the lack of standardisation and consensus on which sequences should be used [11]. 3D fat-suppressed echo MRI sequences provide a high contrast-to-noise ratio between cartilage and subchondral bone [54,55], thus allowing the interface to be clearly assessed. MRI has been shown previously to correlate with cartilage histology [55]. 3D requires a gradient echo sequence and thus there is an increase in the potential for susceptibility artefacts in the follow-up studies; consequently, there is a compromise between the greater degree of resolution obtained in such 3D sequences and the increase in obvious postoperative artefacts. This is of particular relevance in this group of patients, because so many of them have had previous surgical procedures.

The grading scheme used for the MR changes in this study is at best only semiquantitative and may oversimplify and lose information that could be obtained by more sophisticated analysis. Fifty percent of patients had had between one and five procedures on their knee before undergoing ACI grafting. This will obviously influence the MRIs of that joint, often rendering their interpretation more difficult – for example, in defining the edge of the graft to assess the degree of overgrowth or incorporation. The fact that the MRI scores were lower for the patients treated with ACI and mosaicplasty combined almost certainly reflects more interference within the joint for these patients than occurred in patients treated using ACI only. Patients with mosaicplasty as part of their treatment would generally only score 75% of maximum, as they would usually score zero on the subchondral bone parameter.

Several animal studies on ACI have shown that while relatively good cartilage forms initially, it often breaks down and degenerates with time. For example, in dogs [36], the remodelling phase at 3–6 months is followed by a degradative phase, during which the repair tissue and surrounding cartilage appear to become progressively damaged. Results from our studies suggest the opposite may be true in humans treated with ACI, in whom the repair tissue appears to 'mature' with increasing time and tend more towards hyaline cartilage than fibrocartilage [56]. This is similar to the impression obtained from clinical results in long-term follow-up of patients, up to 10 years after ACI [26]. Why there should be this apparent difference in progression between animals and humans is unclear. One common finding in animal studies, however, is delamination of repair tissue from the sur-

rounding 'native' or original cartilage with time [57]. One can imagine that if this occurs, it can only deteriorate further with movement and may be the cause of the subsequent failure of the graft tissue. Observations on patients treated with ACI in this study, and others within our centre, indicate that there is good integration between native and repair tissue. Certainly histological examination demonstrates that the cartilage integrates fully with the underlying bone. Lateral integration is not assessed routinely by the histological samples, because they are taken from the centre of the graft region. However, in the single case where a sample was taken obliquely in a patient treated with ACI and mosaicplasty combined, this showed complete integration across all regions of the sample (see Fig. 1). Lateral integration appears to be good generally, at least in the surface layers, when ascertained by its appearance and resistance to probing at arthroscopy (JB Richardson, unpublished observation).

Why integration might be more successful in humans than other species is unclear. Several factors may contribute, such as the way certain aspects of the procedure are performed – for example, where and how the periosteum is obtained or fixed in place. Alternatively, the type or amount of loading and mobilisation post-treatment may prove to be influential. For example, limited mobilisation, which may be easier to control in patients than in animal models, may be important immediately postoperation in allowing protection of the surgical site in the early weeks. In addition, cells can be mechanically induced to transfer from fibroblastic to chondrocytic cells, at least in tendon [58], and synthesis of proteins and proteoglycans by cartilage cells is inhibited by static compression but not by intermittent loading [59]. Other, more basic, differences between animal species and mankind may be important, such as variations in cartilage thickness, cellularity, or mechanical properties [6].

In summary, we have used histology and MR imaging in an attempt to assess objectively the quality and hence success of ACI in eliciting repair of articular cartilage. Despite more than 6000 ACI procedures being carried out worldwide, the understanding of the biology of cartilage repair remains poor. Further long-term study of patients treated with ACI, together with the use of objective outcome measures, should improve this understanding, and is vital in allowing comparison of the long-term success of this technique with others such as debridement and subchondral drilling for the treatment of cartilage defects. It is only after true objective and scientific study [7] or after the completion of randomised trials [5] that informed judgements on the effectiveness of ACI can be made. In addition, establishing objective, standarised outcome measures will be important to compare and assess future generations of treatment regimes incorporating scaffolds and support matrices, or other, more advanced, tissue-engineered therapies.

Conclusion

Treatment of cartilage defects can result in repair tissue of varying morphology, ranging from predominantly hyaline (22% of biopsy specimens), through mixed (48%), to predominantly fibrocartilage (30% of specimens). Repair tissue averaged 2.5 mm in thickness and appeared to improve with increasing time postgraft. It was well integrated with the host tissue in all aspects viewed. In patients treated with ACI alone, there was a correlation between the histology and MRI scores ($P = 0.02$). We suggest that MRI provides a useful assessment of properties of the whole graft area and adjacent tissue and is a noninvasive technique for long-term follow-up.

Acknowledgements

We are grateful to Drs S Ayad, Manchester, and A Kwan, Cardiff, for the provision of antibodies to collagen types VI and X, respectively; to Professor B Caterson, Cardiff, for all the proteoglycan antibodies; to Mrs Janet Gardiner, Department of Diagnostic Imaging, Robert Jones and Agnes Hunt Orthopaedic Hospital NHS Trust, Oswestry; to Dr J Herman Kuiper for statistical advice; and to other members of OsCell (B and IK Ashton, A Bailey, N Goodstone, D Rees, S Roberts, S Roberts, R Spencer Jones, J Taylor, S Turner, L van Niekerk). The Arthritis Research Campaign has generously provided financial support.

References

1. Brittberg M, Lindahl A, Nilsson A, Ohlsson C, Isaksson O, Peterson L: **Treatment of deep cartilage defects in the knee with autologous chondrocyte transplantation.** *N Engl J Med* 1994, **331**:889-895.
2. Bentley G, Minas T: **Treating joint damage in young people.** *BMJ* 2000, **320**:1585-1588.
3. Buckwalter JA: **Articular cartilage: injuries and potential for healing.** *J Orthop Sports Phys Ther* 1998, **28**:192-202.
4. Minas T, Nehrer S: **Current concepts in the treatment of articular cartilage defects.** *Orthopedics* 1997, **20**:525-536.
5. Jobanputra P, Parry D, Fry-Smith A, Burls A: **Effectiveness of autologous chondrocyte transplantation for hyaline cartilage defects in knee.** *Health Technology Assessment* 2001, **5**:1-57.
6. Buckwalter J: **Evaluating methods of restoring cartilaginous articular surfaces.** *Clin Orthop* 1999, **367(suppl)**:S224-S238.
7. Schneider U, Breusch SJ, von der Mark K: **Aktueller Stellenwert der autologen Chondrozytentransplantation.** *Z Orthop Ihre Grenzgeb* 1999,**137**:386-392.
8. Bader DL, Kempson GE, Egan J, Gilbey W, Barrett AJ: **The effects of selective matrix degradation on the short-term compressive properties of adult human articular cartilage.** *Biochim Biophys Acta* 1992, **1116**:147-154.
9. Pearce RH, Thompson JP, Bebault GM, Flak B: **Magnetic resonance imaging reflects the chemical changes of aging degeneration in the human intervertebral disk.** *J Rheum* 1991, **18**: 42-43.
10. Potter K, Butler JJ, Horton WE, Spencer RGS: **Response of engineered cartilage tissue to biochemical agents as studied by proton magnetic resonance microscopy.** *Arthritis Rheum* 2000, **43**:1580-1590.
11. Recht M, Bobic V, Burstein D, Disler D, Gold G, Gray M, Kramer J, Lang P, McCauley T, Winalski C: **Magnetic resonance imaging of articular cartilage.** *Clin Orthop* 2001, **391(suppl)**: S379-S396.
12. Richardson JB, Caterson B, Evans EH, Ashton BA, Roberts S: **Repair of human articular cartilage after implantation of autologous chondrocytes.** *J Bone Joint Surg Br* 1999, **81**:1064-1068.
13. Harrison PE, Aston IK, Johnson WEB, Turner SL, Richardson JB, Ashton BA: **The *in vitro* growth of human chondrocytes.** *Cell Tissue Banking* 2000, **1**:1-6.
14. Talkhani IS, Richardson JB: **Knee diagram for the documentation of arthroscopic findings of the knee – cadaveric study.** *Knee* 1999, **6**:95-101.

15. Gold GE, Bergman AG, Pauly JM, Lang P, Butts RK, Beaulieu CF, Hargreaves B, Frank L, Boutin RD, Macovski A, Resnick D: **Magnetic resonance imaging of knee cartilage repair.** *Top Magn Res Imaging* 1998, **9**:377-392.
16. Kwan APL, Dickson IR, Freemont AJ, Grant ME: **Comparative studies of type X collagen expression in normal and rachitic chicken epiphyseal cartilage.** *J Cell Biol* 1989, **109**:1849-1856.
17. Poole CA, Ayad S, Schofield JR: **Chondrons from articular cartilage: immunolocalisation of type VI collagen in the pericellular capsule of isolated canine tibial chondrons.** *J Cell Sci* 1988, **90**:635-643.
18. Caterson B, Griffin J, Mahmoodian F, Sorrell JM: **Monoclonal antibodies against chondroitin sulphate isomers: their use as probes for investigating proteoglycan metabolism.** *Biochem Soc Trans* 1990, **18**:820-821.
19. Caterson B, Christner JE, Baker JR, Couchman JR: **Production and characterization of monoclonal antibodies directed against connective tissue proteoglycans.** *Fed Proc* 1985, **44**: 386-393.
20. Sorrell JM, Mahmoodian F, Schafer IA, Davis B, Caterson B: **Identification of monoclonal antibodies that recognise novel epitopes in native chondrotin/dermatan sulfate glycosaminoglycan chains. Their use in mapping functionally distinct domains of human skin.** *J Histochem Cytochem* 1990, **38**:393-402.
21. Caterson B, Christner JE, Baker JR: **Identification of a monoclonal antibody that specifically recognizes corneal and skeletal keratan sulfate.** *J Biol Chem* 1983, **258**:8848-8854.
22. Caterson B, Calabro T, Donohue PJ, Jahnke MR: **Monoclonal antibodies against cartilage proteoglycan and link protein.** In *Articular Cartilage Biochemistry*. Edited by Kuettner KE, Schleyerbach R, Hascall VC. New York: Raven Press; 1986: 59-73.
23. Roberts S, Menage J, Duance VC, Wotton S, Ayad S: **Collagen types around the cells of the intervertebral disc and cartilage end plate: an immunolocalization study.** *Spine* 1991, **16**:1030-1038.
24. Roberts S, Caterson B, Evans EH, Eisenstein SM: **Proteoglycan components of the intervertebral disc and cartilage endplate: an immunolocalization study of animal and human tissues.** *Histochem J* 1994, **26**:402-411.
25. Shrout PE, Fleiss JL: **Intraclass correlations: uses in assessing rater reliabilty.** *Psychol Bull* 1979, **86**:420-428.
26. Peterson L, Minas T, Brittberg M, Nilsson A, Sjorgren-Jansson E, Lindahl A: **two- to 9- year outcome after autologous chondrocyte transplantation of the knee.** *Clin Orthop* 2000, **374**:212-234.
27. Brittberg M, Tallheden T, Sjorgren-Jansson E, Lindahl A, Peterson L: **Autologous chondrocytes used for articular cartilage repair.** *Clin Orthop* 2001, **391(suppl)**:S337-S348.
28. Newman AP: **Articular cartilage repair.** *Am J Sport Med* 1998, **26**:309-324.
29. O'Driscoll SW, Keeley FW, Salter RB: **The chondrogenic potential of free autogenous periosteal grafts for biological resurfacing of major full-thickness defects in joint surfaces under the influence of continuous passive motion.** *J Bone Joint Surg Am* 1986, **68**:1017-1035.
30. O'Driscoll SW, Marx RG, Beaton DE, Miura Y, Gallay SH, Fitzsimmons JS: **Validation of a simple histological, histochemical cartilage scoring system.** *Tissue Eng* 2001, **7**:313-320.
31. Pineda S, Pollack A, Stevenson S, Goldberg V, Caplan A: **A semiquantative scale for histologic grading of articular cartilage repair.** *Acta Anat* 1992, **143**:335-340.
32. Wakitani S, Goto T, Pineda S, Young RG, Mansour JM, Caplan AI, Goldberg VM: **Mesenchymal cell-based repair of large, full-thickness defects of articular cartilage.** *J Bone Joint Surg Am* 1994, **76**:579-592.
33. Ben-Yishay A, Grande DA, Schwartz RE, Menche D, Pitman MD: **Repair of articular cartilage defects with collagen-chondrocyte allografts.** *Tissue Eng* 1995, **1**:119-133.
34. Caplan AI, Elyaderani M, Mochizuki Y, Wakitani S, Goldberg VM: **Principles of cartilage repair and regeneration.** *Clin Orthop* 1997, **342**:254-269.
35. Carranza-Bencano A, Perez-Tinao M, Ballesteros-Vazquez P, Armas-Padron JR, Hevia-Alsono A, Martos Crespo F: **Comparative study of the reconstruction of articular cartilage defects with free costal perichondrial grafts and free tibial periosteal grafts: an experimental study on rabbits.** *Calcif Tissue Int* 1999, **65**:402-407.
36. Breinan HA, Minas T, Barone L, Tubo R, Hsu H-P, Shortkroff S, Nehrer S, Sledge CB, Spector M: **Histological evaluation of the course of healing of canine articular cartilage defects treated with cultured autologous chondrocytes.** *Tissue Eng* 1998, **4**: 101-114.
37. Mankin HJ, Dorfman H, Lippiello L, Zarins A: **Biochemical and metabolic abnormalities in articular cartilage from osteoarthritic human hips.** *J Bone Joint Surg Am* 1971, **53**:523-537.
38. Ostergaard K, Andersen CB, Petersen J, Bendtzen K, Salter DM: **Validity of histopathological grading of articular cartilage from osteoarthritic knee joints.** *Ann Rheum Dis* 1999, **58**:208-213.
39. Grande DA, Breitbart AS, Mason J, Paulino C, Laser J, Schwartz RE: **Cartilage tissue engineering: current limitations and solutions.** *Clin Orthop* 1999, **367(suppl)**:S167-S185.
40. Ratcliffe A, Mow VC: **Articular cartilage.** In *Extracellular Matrix. Volume 1, Tissue Function.* Edited by Comper WD. Amsterdam: Harwood Academic Press; 1996:234-302.
41. Roberts S: **Collagen of the calcified layer of human articular cartilage.** *Experientia* 1985, **41**:1138-1139.
42. Eyre DR, Muir H: **Quantitative analysis of Types I and II collagens in human intervertebral discs at various ages.** *Biochim Biophys Acta* 1977, **492**:29-42.
43. Wotton SF, Duance VC: **Type III collagen in normal human articular cartilage.** *Histochem J* 1994, **26**:412-416.
44. Pullig O, Weseloh G, Swoboda B: **Expression of type VI collagen in normal and osteoarthritic human cartilage.** *Osteoarthritis Cartilage* 1999, **7**:191-202.
45. Rucklidge GJ, Milne G, Robins SP: **Collagen type X: a component of the surface of normal human, pig and rat articular cartilage.** *Biochem Biophys Res Comm* 1996, **224**:297-302.
46. von der Mark K, Kirsch T, Nerlich A, Kuss A, Weseloh G, Glückert K, Burkhardt HS: **Type X collagen synthesis in human osteoarthritic cartilage.** *Arthritis Rheum* 1992, **35**:806-811.
47. Wardale RJ, Duance VC: **Characterization of articular and growth plate cartilage collagens in porcine osteochondrosis.** *J Cell Sci* 1994, **107**:47-59.
48. Roberts S, Bains MA, Kwan A, Menage J, Eisenstein SM: **Type X collagen in the human intervertebral disc: an indication of repair or remodelling?** *Histochem J* 1998, **30**:89-95.
49. Takahashi I, Mizoguchi I, Sasano Y, Saitoh S, Ishida M, Kagayama M, Mitani H: **Age-related changes in the localization of glycosaminoglycans in condylar cartilage of the mandible in rats.** *Anat Embryol* 1996, **194**:489-500.
50. Nakano T, Dodd CM, Scott PG: **Glycosaminoglycans and proteoglycans from different zones of the porcine knee meniscus.** *J Orthop Res* 1997, **15**:213-222.
51. Caterson B, Mahmoodian F, Sorrell JM, Hardingham TE, Bayliss MT, Ratcliffe A, Muir H: **Modulation of native chondroitin sulphate structure in tissue development and in disease.** *J Cell Sci* 1990, **97**:411-417.
52. Lin PP, Buckwater JA, Olmstead M, Caterson B: **Expression of proteoglycan epitopes in articular cartilage repair tissue.** *Iowa Orthop J* 1998, **18**:12-18.
53. Chung CB, Frank LR, Resnick D: **Magnetic resonance imaging: state of the art. Cartilage imaging techniques. Current clinical applications and state of the art imaging.** *Clin Orthop* 2001, **391(suppl)**:S370-S376.
54. Disler DG, McCauley TR, Wirth CR, Fuchs MD: **Detection of knee hyaline cartilage defects using fat-supressed three-dimensional spoiled gradient-echo MR imaging: comparison with standard MR imaging and correlation with arthroscopy.** *AJR Am J Roentgenol* 1995, **165**:377-382.
55. Trattnig S, Huber M, Breitenseher MJ, Trnka H-J, Rand T, Kaider A, Helbich T, Imhof H, Resnick D: **Imaging articular cartilage defects with 3D fat-suppressed echo planar imaging: comparison with conventional 3D supressed gradient echo sequence and correlation with histology.** *J Comput Assist Tomogr* 1998, **22**:8-14.
56. Roberts S, Hollander AP, Caterson B, Menage J, Richardson JB: **Matrix turnover in human cartilage repair tissue in autologous chondrocyte implantation.** *Arthritis Rheum* 2001, **44**:2586-2598.
57. Nehrer S, Breinan HA, Ramappa A, Hsu H-P, Minas T, Shortkroff S, Sledge CB, Yannas IV, Spector M: **Chondrocyte-seeded collagen matrices implanted in a chondral defect in a canine model.** *Biomaterials* 1998, **19**:2313-2328.

58. Ehlers TW, Vogel KG: **Proteoglycan synthesis by fibroblasts from different regions of bovine tendon cultured in alginate beads.** *Comp Biochem Physiol A Mol Integr Physiol* 1998, **121**: 355-363.
59. Burton-Wurster N, Vernier-Singer M, Farquhar T, Lust G: **Effect of compressive loading and unloading on the synthesis of total protein, proteoglycan, and fibronectin by canine cartilage explants.** *J Orthop Res* 1993, **11**:717-729.

Correspondence

S Roberts, Centre for Spinal Studies, Robert Jones and Agnes Hunt Orthopaedic Hospital NHS Trust, Oswestry, Shropshire SY10 7AG, UK. Tel: +44 1691 404664; fax: +44 1691 404054; e-mail: s.roberts@keele.ac.uk